Syndecan-2 induces filopodia and dendritic spine formation via the neurofibromin–PKA–Ena/VASP pathway

Yi-Ling Lin,[1,4] Ya-Ting Lei,[2,4] Chen-Jei Hong,[3,4] and Yi-Ping Hsueh[1,2,3,4]

[1]Faculty of Life Sciences, Institute of Genome Sciences, and [2]Institute of Microbiology and Immunology, National Yang-Ming University, Taipei 112, Taiwan
[3]Graduate Institute of Life Sciences, National Defense Medical Center, Taipei 114, Taiwan
[4]Institute of Molecular Biology, Academia Sinica, Taipei 115, Taiwan

Syndecan-2 induced filopodia before spinogenesis; therefore, filopodia formation was used here as a model to study the early downstream signaling of syndecan-2 that leads to spinogenesis. Screening using kinase inhibitors indicated that protein kinase A (PKA) is required for syndecan-2–induced filopodia formation in both human embryonic kidney cells and hippocampal neurons. Because neurofibromin, a syndecan-2–binding partner, activates the cyclic adenosine monophosphate pathway, the role of neurofibromin in syndecan-2–induced filopodia formation was investigated by deletion mutant analysis, RNA interference, and dominant-negative mutant. The results showed that neurofibromin mediates the syndecan-2 signal to PKA. Among actin-associated proteins, Enabled (Ena)/vasodilator-stimulated phosphoprotein (VASP) were predicted as PKA effectors downstream of syndecan-2, as Ena/VASP, which is activated by PKA, induces actin polymerization. Indeed, when the activities of Ena/VASP were blocked, syndecan-2 no longer induced filopodia formation. Finally, in addition to filopodia formation, neurofibromin and Ena/VASP contributed to spinogenesis. This study reveals a novel signaling pathway in which syndecan-2 activates PKA via neurofibromin and PKA consequently phosphorylates Ena/VASP, promoting filopodia and spine formation.

Introduction

Dendritic spines are small protrusions from the dendrite that form the postsynaptic component of excitatory synapses. Filopodia are recognized as one origin of dendritic spines (for reviews see Hering and Sheng, 2001; Ethell and Pasquale, 2005). During early stages of synaptogenesis, filopodia rapidly protrude and retract from dendrites. When dendritic filopodia contact presynaptic sites and form synapses, filopodia contract and transform into dendritic spines. Many transmembrane receptors and intracellular molecules have been shown to play a role in spinogenesis (for reviews see Hering and Sheng, 2001; Carlisle and Kennedy, 2005; Ethell and Pasquale, 2005; Lippman and Dunaevsky, 2005; Tada and Sheng, 2006), including syndecan-2.

Syndecan-2 belongs to the syndecan family of transmembrane heparan sulfate proteoglycans. By virtue of their heparan sulfate modifications, syndecans act as coreceptors for growth or differentiation factors, presenting these molecules to specific receptor tyrosine kinases, including the fibroblast growth factor receptors (Filla et al., 1998). Syndecans also function as adhesion molecules that regulate cell migration, cell–cell interactions, and cell–extracellular matrix interactions (Klass et al., 2000; Beauvais et al., 2004; Reiland et al., 2004). During neural development, syndecan-2 expression is elevated during synaptogenesis (Ethell and Yamaguchi, 1999; Hsueh and Sheng, 1999a). The overexpression of syndecan-2 starting at 1 d in vitro (DIV) accelerates spine formation in hippocampal neurons examined at 8 DIV (Ethell and Yamaguchi, 1999), suggesting a role of syndecan-2 in spinogenesis. Because syndecan-2 overexpression also promotes filopodia formation in nonneuronal cell lines such as COS-1 and Swiss 3T3 (Granes et al., 1999, 2000), it is possible that syndecan-2 first promotes filopodia formation and, consequently, transforms filopodia into dendritic spines in neurons.

Correspondence to Yi-Ping Hsueh: yph@gate.sinica.edu.tw

Abbreviations used in this paper: CASK, calcium/CaM-dependent serine protein kinase; DIV, day in vitro; Ena, Enabled; EVL, Ena-VASP–like; FSK, forskolin; HEK, human embryonic kidney; Mena, mammalian enabled; NF1, neurofibromatosis type 1; PI3K, phosphatidylinositol 3-kinase; shRNA, small hairpin RNA; VASP, vasodilator-stimulated phosphoprotein.

The online version of this article contains supplemental material.

The Journal of Cell Biology, Vol. 177, No. 5, June 04, 2007 829–841
http://www.jcb.org/cgi/doi/10.1083/jcb.200608121

As yet, the molecular mechanism underlying the effect of syndecan-2 on cytoskeleton rearrangement remains unclear. Although the cytoplasmic domain of syndecan-2 is short (~30 residues) and has no kinase domain, several syndecan-2–interacting proteins have been identified whose activity may provide clues about syndecan-2 signaling. The cytoplasmic domain of syndecan-2 consists of three small regions: two highly conserved regions (C1 and C2) and, between these, a variable (V) region unique to each syndecan. The C2 region contains a type II PDZ-binding motif (residues E-F-Y-A; Cohen et al., 1998; Hsueh et al., 1998). This EFYA motif is important for syndecan-2–dependent dendritic spine formation, and syndecan-2 loses the ability to promote spinogenesis when the C2 motif is removed (Ethell and Yamaguchi, 1999). Several adaptor proteins such as syntenin, calcium/CaM-dependent serine protein kinase (CASK), synbindin, and synectin all bind to the EFYA motif of syndecans (Grootjans et al., 1997; Cohen et al., 1998; Hsueh et al., 1998; Ethell et al., 2000; Gao et al., 2000), suggesting that these interactions play a role in synaptic formation.

Another syndecan-2–interacting protein is neurofibromin (Hsueh et al., 2001), which is encoded by the *neurofibromatosis type 1* (*NF1*) gene and interacts with the C1 region of syndecan-2. 40–60% of NF1 patients are characterized as having specific learning disabilities (for reviews see Rosser and Packer, 2003; Acosta et al., 2006). Mice carrying a heterozygous null mutation of the *NFl* gene also show several features of the learning deficits associated with *NF1* mutations in humans (for review see Costa and Silva, 2002; Costa et al., 2002). These studies indicate an important role of neurofibromin in neuronal function. At the molecular level, neurofibromin possesses a central Ras GTPase-activating protein–related domain that regulates the Ras–MAPK pathway (for reviews see Cichowski and Jacks, 2001; Zhu and Parada, 2001). In addition, neurofibromin is also involved in the cAMP pathway via the regulation of adenylyl cyclase through two distinct pathways (Tong et al., 2002; Dasgupta et al., 2003; Hannan et al., 2006). One is the receptor tyrosine kinase pathway, which acts independently of any heterotrimeric G protein; Ras activation by neurofibromin is essential for this pathway. The other is the classic heterotrimeric G-protein pathway, which is $G\alpha_s$ dependent and requires the C-terminal region of neurofibromin (Hannan et al., 2006).

In this study, we elucidate the role of these intracellular interactions of syndecan-2 in neuronal morphogenesis. Filopodia formation in nonneuronal cells was chosen here as a model to study the early downstream signaling of syndecan-2. The common signaling of the syndecan-2–neurofibromin–PKA–Enabled (Ena)/vasodilator-stimulated phosphoprotein (VASP) pathway leading to filopodia formation and spinogenesis was then studied in cultured hippocampal neurons. Our study provides the first evidence that neurofibromin is required for dendritic spine formation, which may explain how *NF1* mutation leads to deficits in learning and memory.

Results

Syndecan-2 is essential for dendritic spine formation

To confirm that syndecan-2 is important for dendritic spine formation, we used an RNAi approach to reduce neuronal syndecan-2 protein levels. First, we examined the ability of syndecan-2 small hairpin RNA (shRNA) to knock down syndecan-2. Syndecan-2 shRNA but not vector control (SUPER.neo+GFP) efficiently down-regulated syndecan-2 protein expression in both human embryonic kidney (HEK) 293T cells and cultured hippocampal neurons (Fig. S1, A and B; available at http://www.jcb.org/cgi/content/full/jcb.200608121/DC1). The effect of syndecan-2 shRNA on dendritic spine formation was then investigated. Constructs expressing syndecan-2 shRNA (also expressing GFP) and GFP–actin were cotransfected into hippocampal neurons at 11 DIV. Morphology of dendritic protrusions was then assessed by GFP and GFP-actin signals. At 16 DIV, dendritic spines in our cultures had differentiated and exhibited

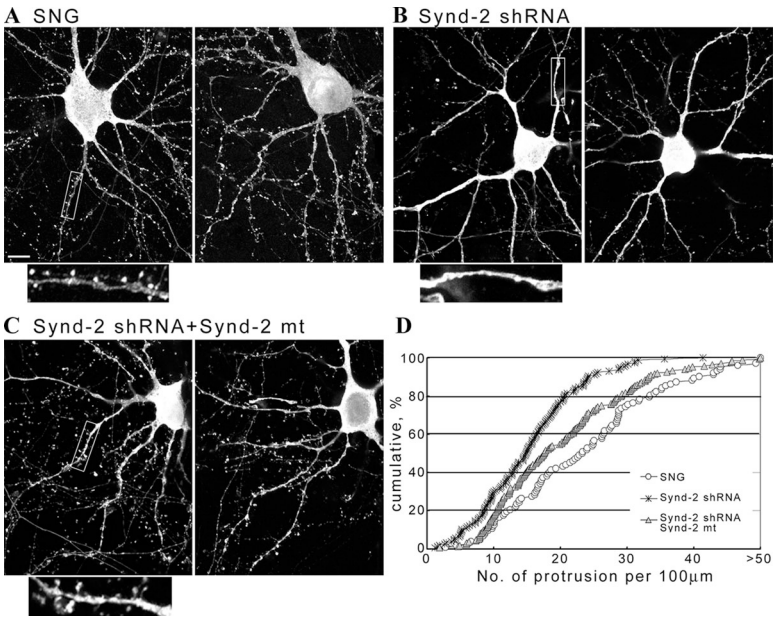

Figure 1. **Syndecan-2 is important for dendritic spine formation.** (A–C) Cultured hippocampal neurons were cotransfected with vector control SNG (pSUPER.neo+GFP) and EGFP-actin (DNA ratio 2:1; A), syndecan-2 shRNA and EGFP-actin (DNA ratio 2:1; B), and syndecan-2 shRNA, EGFP-actin, and syndecan-2 silent mutant resistant to syndecan-2 shRNA (DNA ratio 6:1:6; C). The GFP and GFP-actin signals were then viewed to assess cell morphology. The insets are the magnified images of the boxed areas. Bar, 10 μm. (D) Quantitative analysis of the effects of syndecan-2 shRNA on spine formation as described in Materials and methods. The cumulative probability distributions of protrusion density along dendrites are shown.

characteristics of mature spines (Fig. 1 A, inset). In the presence of syndecan-2 shRNA, the number of dendritic protrusions representing dendritic spines was greatly reduced (Fig. 1, B and D). To ensure the sequence-specific effect of syndecan-2 shRNA, a syndecan-2 silent mutant insensitive to syndecan-2 shRNA was coexpressed with syndecan-2 shRNA (Fig. 1 C). Overexpression of the silent mutant did rescue the effect of syndecan-2 shRNA on protrusion number (Fig. 1 D). In addition, mature spines were observed along the dendrites in the presence of syndecan-2 mutant (Fig. 1 C, inset). These results support a critical role for syndecan-2 in dendritic spine formation.

Because dendritic filopodia have been proposed to be precursors of dendritic spines and syndecan-2 has been shown to induce filopodia formation in nonneuronal cells (Granes et al., 1999, 2000), it is likely that the overexpression of syndecan-2 in cultured hippocampal neurons first induces filopodia formation and then promotes dendritic spine maturation. Indeed, when syndecan-2 was transfected into cultured hippocampal neurons at 1 DIV, numerous filopodia emerging from dendrites were observed at 4–5 DIV (Fig. 2 C). Because filopodia formation induced by syndecan-2 also occurs in nonneuronal cells, this initial process involved in dendritic spinogenesis does not appear to be neuron specific, although the transformation from filopodia to spines should be specific for neurons. To explore the signaling downstream of syndecan-2 that initiates spine formation, we first used filopodia formation in nonneuronal HEK cells as a model system for syndecan signaling and confirmed these observations in cultured hippocampal neurons.

Downstream signaling of syndecan-2

To monitor syndecan-2 expression and cell morphology of transfected cells, we generated the syndecan-2 antibody syndecan-2G.

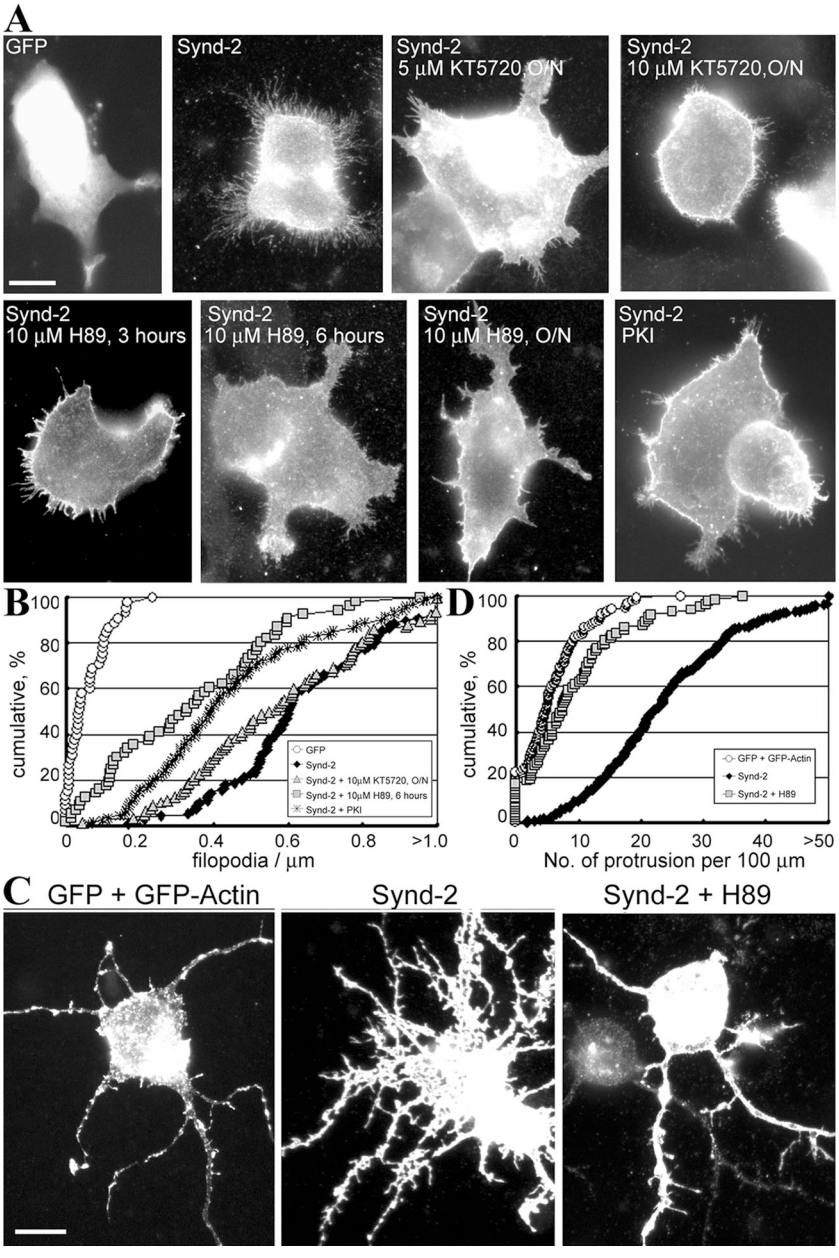

Figure 2. **PKA is involved in syndecan-2–induced filopodia formation.** (A) HEK293T cells were transfected with GFP, syndecan-2, or PKI construct as indicated. For cells transfected with syndecan-2, immunostaining using the syndecan-2G antibody was performed. For cells transfected with GFP, immunostaining was skipped. PKA inhibitors KT5720 and H89 were added to the culture 16 (O/N), 6, or 3 h before harvesting as indicated. (B) Cumulative probability distributions of filopodia density in A were analyzed as described in Materials and methods. (C) PKA is involved in syndecan-2–induced filopodia in neurons. Syndecan-2, GFP, and GFP-actin were transfected into cultured hippocampal neurons at 1 DIV. 3–4 d later, cells were fixed and subjected to immunostaining. H89 (at a final concentration of 10 μM) was added 12 h before harvest. (D) Cumulative probability distributions of the filopodia density in C. Bars, 10 μm.

This antibody was confirmed as recognizing syndecan-2 (Fig. S2, A and B; available at http://www.jcb.org/cgi/content/full/jcb.200608121/DC1) but not syndecan-1, -3, or -4 (Fig. S2 A) in both immunoblotting and immunostaining experiments in transfected COS cells, confirming its high syndecan-2 specificity.

Generally, there are very few filopodia on the surface of parental HEK cells (<0.2 filopodia per μm; Fig. 2 B). When syndecan-2 was overexpressed in HEK293T cells, numerous filopodia were revealed by syndecan-2G antibody (Fig. 2 A). Cotransfection of syndecan-2 and GFP into HEK cells was also performed (unpublished data). Perhaps as a result of staining of the plasma membrane, we found that syndecan-2 signal outlined the morphology of HEK cells more clearly than GFP signal. To explore the downstream signaling of syndecan-2, several kinase inhibitors were added to cultures overexpressing syndecan-2, including the phosphatidylinositol 3-kinase (PI3K) inhibitors LY294002 and wortmannin, PKC inhibitors Go6976 and Go6850, and PKA inhibitors KT5720 and H89. Neither PIK3 nor PKC inhibitors prevented filopodia formation induced by syndecan-2 (Fig. S3, available at http://www.jcb.org/cgi/content/full/jcb.200608121/DC1), suggesting that syndecan-2–induced filopodia formation is independent of the PI3K–Akt and PKC pathways. In contrast, both PKA inhibitors KT5720 and H89 decreased syndecan-2–induced filopodia formation (Fig. 2, A and B), although the effect of KT5720 was weaker than that of H89 for unknown reasons. To further confirm that PKA is involved in syndecan-2 signaling, a construct expressing the PKA-specific peptide inhibitor PKI was cotransfected with syndecan-2 into HEK cells. The presence of PKI significantly reduced the filopodia density on the surface of syndecan-2–expressing HEK293T cells ($P < 0.001$; Fig. 2, A and B), supporting the idea that PKA signaling is important for syndecan-2–induced filopodia formation in HEK293T cells.

Results for cultured hippocampal neurons were similar to those in HEK293T cells: PKA inhibitor H89 efficiently reduced the number of syndecan-2–induced filopodia along neurites (Fig. 2, C and D). These results indicated that syndecan-2 induces dendritic filopodia formation via PKA in cultured hippocampal neurons.

Involvement of the syndecan-2 C1 region in filopodia formation

A series of C-terminal mutants of syndecan-2 (Fig. 3 A) were then used to map the cytoplasmic regions of syndecan-2 that are required for filopodia formation. Mutant genes were transfected into HEK293T cells, and immunoblotting with syndecan-2G antibody confirmed that expression levels of these mutants were comparable with those of wild-type syndecan-2 (Fig. S2 C). In addition, these deletions did not considerably affect the plasma membrane targeting of mutants (unpublished data). The effects of these mutants on filopodia formation in HEK293T cells were then examined. The mutant syndecan-2Δ3 lacking the last three residues of syndecan-2 successfully induced normal filopodia formation (Fig. 3, B and C). The ability of the mutant syndecan-2Δ20 lacking the cytoplasmic V and C2 regions to induce filopodia was slightly weaker than that of wild-type syndecan-2 (Fig. 3, B and C). When the entire cytoplasmic region of syndecan-2 was

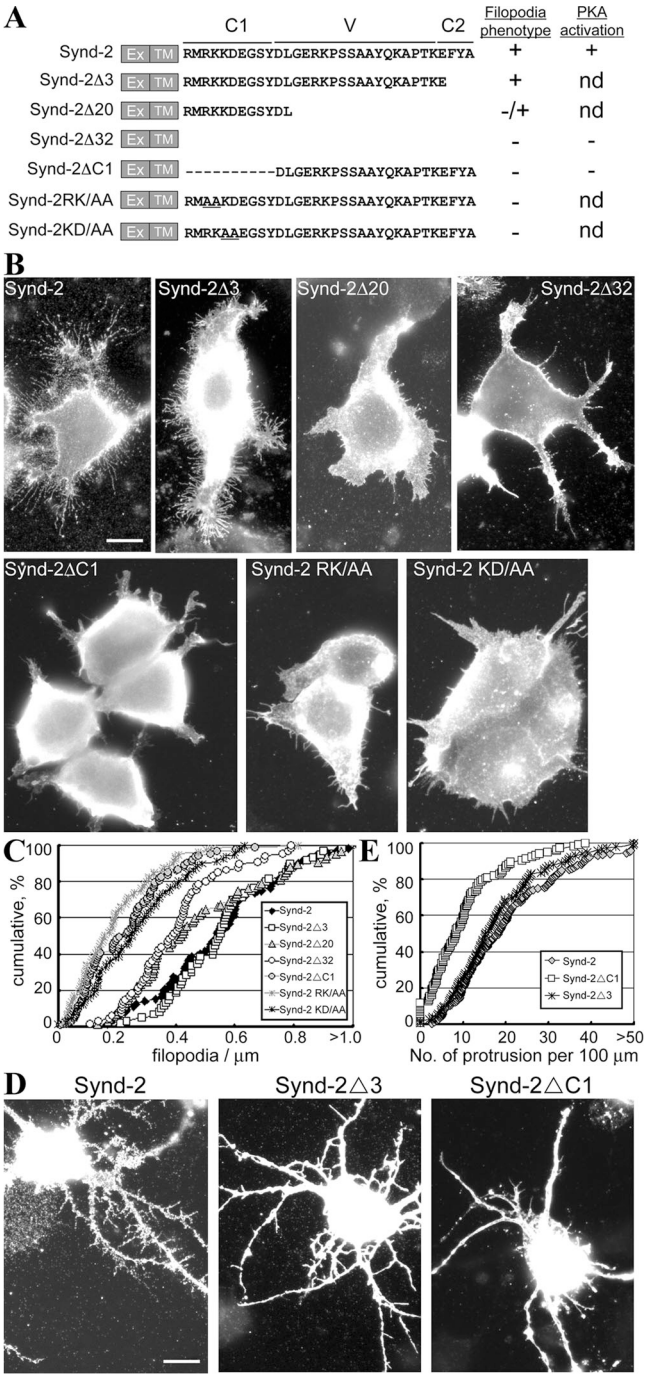

Figure 3. **The syndecan-2 cytoplasmic C1 region is critical for filopodia formation.** (A) Amino acid sequences of the rat syndecan-2 constructs. The sequences of extracellular (Ex) and transmembrane (TM) domains are not shown because of space constraints. The underlining indicates the C1, V, and C2 regions. The abilities of each construct to induce filopodia formation and PKA activation are summarized at the right. (B) Wild-type syndecan-2 and a series of C-terminal deletion mutants were separately transfected into HEK293T cells. Cell morphology was then examined by immunofluorescent staining using the syndecan-2G antibody. (C) Cumulative probability distributions of the filopodia density in B. (D) Cultured hippocampal neurons were transfected with wild-type syndecan-2, -2Δ3, and -2ΔC1. Cell morphology of transfected neurons was analyzed by immunostaining using syndecan-2G antibody. (E) Cumulative probability distributions of the filopodia density in D. Bars, 10 μm.

removed in the syndecan-2Δ32 mutant, the ability to form filopodia was greatly impaired (Fig. 3, B and C). In the syndecan-2ΔC1 mutant lacking only the C1 region, the ability to promote filopodia formation was also greatly reduced (Fig. 3, B and C). These results suggested that both the C1 and V regions (variable region of syndecan) of syndecan-2 are involved in filopodia formation in HEK cells, with the C1 region being the most critical.

To confirm the role of the syndecan-2 C1 region in dendritic filopodia formation, wild-type syndecan-2, -2ΔC1, and -2Δ3 mutants were transfected into cultured hippocampal neurons. Compared with wild-type syndecan-2, the number of dendritic filopodia was greatly reduced in neurons expressing syndecan-2ΔC1 (Fig. 3, D and E). In contrast, syndecan-2Δ3 still efficiently induced dendritic filopodia formation (Fig. 3, D and E). These data supported the notion that the C1 region is also critical for syndecan-2–induced filopodia formation in neurons.

Because the C1 region of syndecan-2 is the most important region for neurofibromin interaction and neurofibromin is involved in both neurite outgrowth (Yunoue et al., 2003) and cAMP signaling, we investigated whether the interaction of neurofibromin with the C1 region of syndecan-2 mediates signaling from syndecan-2 to PKA. Because mutation of the RKKD motif in the C1 region of syndecan-2 impairs neurofibromin interaction (Hsueh et al., 2001), we explored this possibility by examining the effects of the alanine replacement mutants syndecan-2 RK/AA and KD/AA on filopodia formation. Indeed, the ability of syndecan-2 RK/AA and KD/AA mutants to induce filopodia formation was much weaker than that of wild type (Fig. 3, B and C), suggesting that an interaction with neurofibromin is involved in filopodia formation induced by syndecan-2.

Dynamic analysis of filopodia

In addition to characterizing filopodia density, we also dynamically analyzed filopodia behavior using time-lapse techniques. For syndecan-2–induced filopodia, the motility of filopodia was generally very low. The length of most filopodia did not change substantially during the time recorded (around 10 min; Fig. 4 A): only a small fraction of filopodia was altered in length, with a mean velocity of 1.55 ± 0.42 μm/min (Fig. 4 B). In contrast, the motility of syndecan-2ΔC1–expressing cells was higher. Syndecan-2ΔC1–induced filopodia frequently extended and withdrew at greater amplitudes (Fig. 4 A) and at a mean velocity of 1.86 ± 0.39 μm/min (Fig. 4 B). The majority (12 out of 15) of syndecan-2ΔC1–induced filopodia extended or withdrew their tips to lengths >1 μm within 6 min (Fig. 4 C, middle; red lines). In contrast, only the minority (3 out of 12) of mobile syndecan-2–induced filopodia exhibited this ability (Fig. 4 C, top; red lines). When forskolin (FSK), which increases cAMP levels, was added into culture transfected with syndecan-2ΔC1, filopodia movement was immediately frozen (Fig. 4, A and C); only a small fraction still extended or withdrew with a mean velocity of 1.29 ± 0.26 μm/min (Fig. 4 B), and the movement amplitude was <1 μm within 6 min (Fig. 4 C, bottom). These results indicated that syndecan-2–induced filopodia are very stable and that the PKA pathway may play an important role in stabilizing formed filopodia. The relative instability of syndecan-2ΔC1–induced filopodia may account for the lower filopodia density shown in Fig. 3 (B and C).

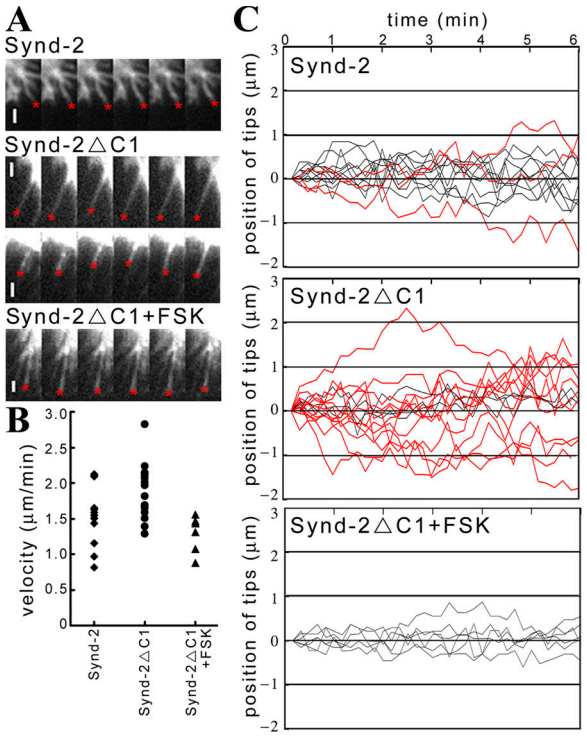

Figure 4. **Time-lapse analysis of filopodia growth in HEK293T cells.** Syndecan-2 and -2ΔC1 mutants were cotransfected with GFP-actin. 18 h after transfection, cells were subjected to time-lapse analysis. Dynamics of filopodia were monitored by GFP-actin signals. Images were taken every 10 s. For syndecan-2ΔC1–expressing cells, after a 10-min recording, forskolin (FSK) was added into the chamber, and cell morphology was recorded for 10 more minutes. (A) The representative images for each group. The intervals between each image shown are 1 min. Red asterisks indicate the tips of filopodia. Bars, 1 μm. (B) The elongation/withdraw rate of filopodia. Each spot indicates one filopodia behavior. (C) Relative positions of filopodia tips during the 6-min recording. The tip that moved a distance of >1 μm within 6 min is marked in red.

Overexpression of syndecans activates PKA

The aforementioned experiments demonstrated that syndecan-2–induced filopodia formation was prevented by the addition of PKA inhibitors. Thus, it is possible that the overexpression of syndecan-2 activates PKA and subsequently promotes filopodia formation. To test this possibility, we compared PKA activity (measured by ELISA) between cells transfected with syndecan-2 or with control vector. Syndecan-2 overexpression in HEK293T cells resulted in 20–30% increases in total PKA activity compared with the vector control (Fig. 5). The mutant syndecan-2Δ32, which lacked the entire cytoplasmic domain of syndecan-2, lost the ability to enhance PKA activity (Fig. 5). The syndecan-2ΔC1 mutant missing the critical C1 region was also unable to activate PKA (Fig. 5). These results support a model for syndecan-2 activation of PKA via its cytoplasmic C1 region, culminating in filopodia formation.

Neurofibromin is required for filopodia formation induced by syndecan-2

To confirm that neurofibromin mediates signaling from syndecan-2 to PKA, leading to filopodia formation, we used two approaches.

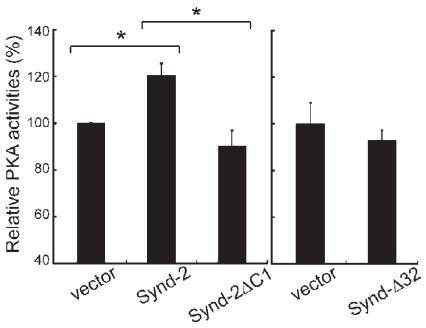

Figure 5. **Syndecan-2 overexpression activates PKA in HEK293T cells.** HEK293T cells were transfected with syndecan-2 constructs and the vector control as indicated and were harvested for PKA activity assays 18 h after transfection. Data shown are the mean ± SEM (error bars) of relative PKA activities. Statistical analysis was performed by one-way analysis of variance to evaluate the difference between the vector control and the specific construct (*, $P < 0.05$; $n = 5$).

The first approach was to interrupt the interaction between neurofibromin and syndecan-2 by overexpression of the syndecan-2–interacting domain of neurofibromin, the Jn fragment (residues 1,356–1,473), which was identified in a yeast two-hybrid assay (Hsueh et al., 2001). Interaction between syndecan and neurofibromin Jn fragments was first confirmed under mammalian cell culture conditions using coimmunoprecipitation (Fig. S1 D). The effect of the Jn fragment on syndecan-2–induced filopodia formation was then examined. When the Jn fragment was overexpressed, filopodia formation induced by syndecan-2 was greatly reduced in HEK293T cells (Fig. 6 A). More important, the Jn fragment also inhibited filopodia formation in cultured hippocampal neurons (Fig. 6, B and C), suggesting an essential role for the interaction between syndecan-2 and neurofibromin in syndecan-2–induced filopodia formation. Overexpression of the Jn fragment alone did not cause an obvious morphological abnormality of cultured neurons. Neither dendrite number nor the length of dendrites was affected by the Jn fragment (unpublished data), supporting the specific effect of the Jn fragment on syndecan-2–induced filopodia formation. If interrupting the interaction between syndecan-2 and neurofibromin by adding the Jn fragment prevents PKA activation and, thus, blocks filopodia formation, it can be predicted that increasing PKA activity in Jn-expressing cells should restore filopodia formation. Indeed, the addition of FSK restored filopodia formation impaired by the Jn fragment in both HEK293T cells (Fig. 6 A) and cultured hippocampal neurons (Fig. 6, B and C).

The second approach to investigate the role of neurofibromin in syndecan-2–induced filopodia formation was to down-regulate endogenous neurofibromin expression by RNAi. We first examined the down-regulation of endogenous NF1 expression using an NF1 shRNA construct (Fig. S1 C). When syndecan-2 and NF1 shRNA construct were cotransfected into HEK cells, the filopodia density was significantly reduced ($P < 0.001$; Fig. 7 A). Similarly, the expression of NF1 shRNA in cultured hippocampal neurons impaired dendritic filopodia formation compared with nonsilencer control (Fig. 7, B and C). Again, to confirm that the effect of NF1 shRNA is to block the signaling from syndecan-2 to the cAMP–PKA pathway, FSK was added into the cultures transfected with syndecan-2 and NF1 shRNA construct. Adding FSK completely restored the filopodia formation in both HEK cells and hippocampal neurons (Fig. 7). These results supported the notion that neurofibromin mediates signaling to the cAMP–PKA pathway that is required for syndecan-2–induced filopodia formation in neurons.

The aforementioned study demonstrated that PKA is the important downstream effector of syndecan-2 on the induction of filopodia formation. We then wondered whether the activation of PKA alone is sufficient for filopodia formation in cultured hippocampal neurons. To address this point, FSK and dibutyryl cAMP were added into young hippocampal neurons

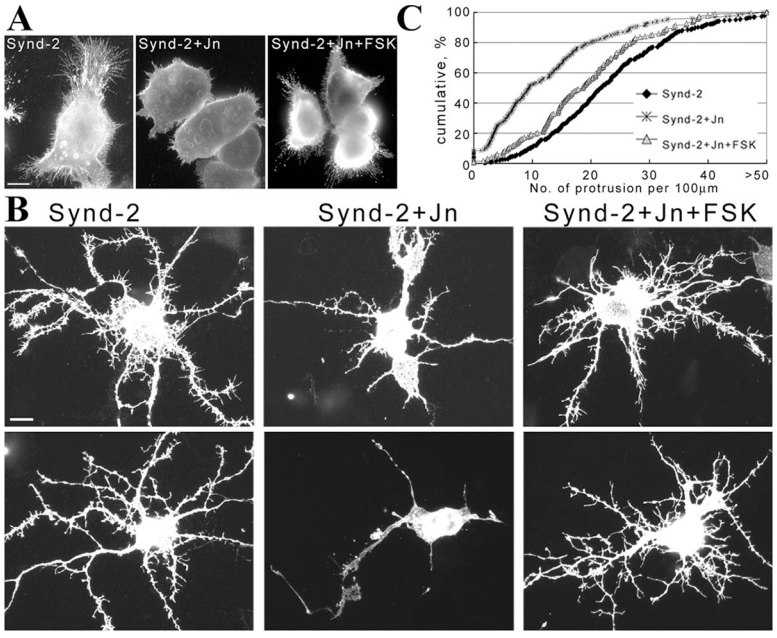

Figure 6. **Disruption of the interaction between syndecan and neurofibromin prevents syndecan-induced filopodia formation.** (A and B) Syndecan-2 was cotransfected with the HA-Jn fragment or vector control into HEK293T cells (A) and 1-DIV cultured hippocampal neurons (B). FSK (20 μM for HEK cells and 75 μM for neurons) was added to the culture 16 (A) or 12 (B) h before harvest for immunostaining using syndecan-2G and HA antibodies. Only the syndecan-2 staining patterns are shown. Bars, 10 μm. (C) Cumulative probability distributions of the filopodia density in B.

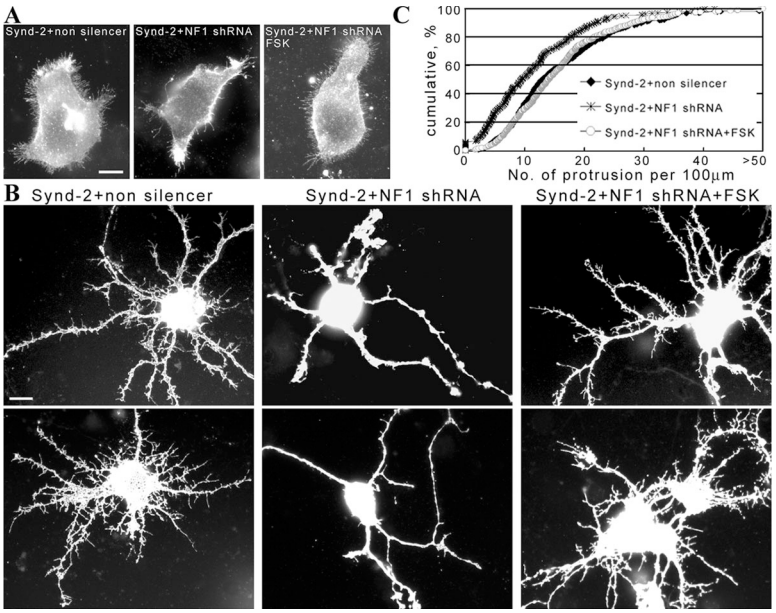

Figure 7. **Knocking down of endogenous neurofibromin prevents syndecan-2–induced filopodia formation.** (A and B) HEK293 cells (A) and cultured hippocampal neurons (B) were transfected with syndecan-2, the NF1 shRNA, and nonsilencer control as indicated. The ratio of syndecan-2 cDNA to shRNA construct was 1:2. FSK was added to the cultures to access the effect of neurofibromin on PKA. (C) Cumulative probability distributions of the filopodia densities in B. Bars, 10 μm.

(5 DIV) without the overexpression of syndecan-2. The results showed that FSK and dibutyryl cAMP could not induce filopodia formation in the absence of syndecan-2 (Fig. 8), suggesting that although PKA is required for syndecan-2–induced filopodia formation, activation of PKA alone is not sufficient for filopodia formation. Multiple signaling provided by syndecan-2 may be involved in filopodia formation.

Ena/VASP proteins contribute to syndecan-2–induced filopodia formation

We then addressed how PKA conducts the signal from syndecan-2/neurofibromin to induce cytoskeleton rearrangement. Previous studies had demonstrated that Ena/VASP proteins, which are important for the formation and elongation of filopodia, are regulated by PKA phosphorylation (Aszodi et al., 1999; Hauser et al., 1999; Lebrand et al., 2004). There are three related Ena/VASP proteins in vertebrates—mammalian enabled (Mena), VASP, and Ena-VASP–like (EVL)—that are highly related and can function interchangeably (Laurent et al., 1999; Geese et al., 2002; Loureiro et al., 2002). They promote actin filament elongation by interacting with barbed ends and shielding them from capping proteins (Bear et al., 2002). Mena, EVL, and VASP all share a conserved PKA phosphorylation site, which is critical for the regulation of their function in actin filament elongation (Loureiro et al., 2002). It has been shown that Mena is present at the tip of growth cone filopodia (Lanier et al., 1999), where it is positioned to initiate actin polymerization and promote filopodia elongation.

To address whether Ena/VASP is the downstream effector of the syndecan-2–neurofibromain–PKA pathway, we first examined whether Ena/VASP proteins are present at the tips of syndecan-2–induced filopodia. GFP-Mena, -VASP, and -EVL all distributed to the tips of every single filopodia in syndecan-2–transfected HEK293T cells (Fig. S4 A, available at http://www.jcb.org/cgi/content/full/jcb.200608121/DC1) as well as cultured neurons (Fig. 9 A). These results favor the possibility that

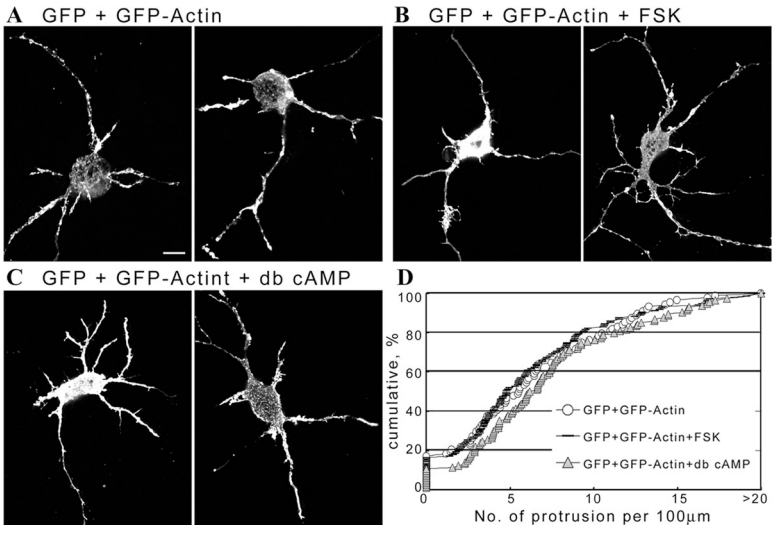

Figure 8. **PKA activation alone does not considerably enhance dendritic filopodia formation in cultured hippocampal neurons.** (A–C) GFP and GFP-actin expression constructs were cotransfected into cultured hippocampal neurons at 1 DIV. At 5 DIV, cells were fixed for monitoring morphology. (B and C) 12 h before fixation, FSK (B) and dibutyryl cAMP (db cAMP; C) were added into the cultures at a final concentration of 75 μM and 1 mM, respectively. (D) Cumulative probability distributions of the filopodia density in A–C. Bar, 10 μm.

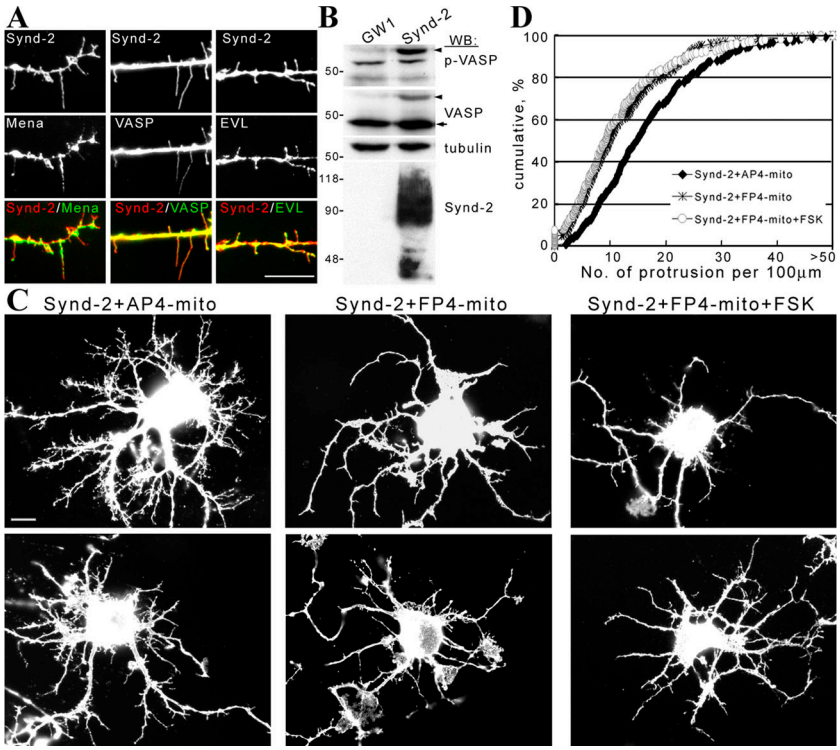

Figure 9. **Ena/VASP proteins are important for syndecan-2 signaling in filopodia formation.** (A) Syndecan-2 was cotransfected with EGFP-Mena, -VASP, and -EVL into cultured hippocampal neurons at 1 DIV. Cells were harvested for staining using syndecan-2G and GFP antibodies at 4–5 DIV. Syndecan-2 was viewed by AlexaFluor594 in red; Ena/VASP proteins were viewed by AlexaFluor488 in green. (B) Syndecan-2 overexpression induces VASP phosphorylation. HEK cells were transfected with syndecan-2 and vector control and subjected to immunoblotting using antibodies recognizing phosphorylated S157 and S239 of VASP and other proteins as indicated. Arrowheads point to phosphorylated VASP; the arrow points to unphosphorylated VASP. (C) Syndecan-2 was cotransfected with the AP4-mito or FP4-mito construct into cultured hippocampal neurons. Filopodia formation was monitored using the syndecan-2 staining pattern. (D) Cumulative probability distributions of the filopodia density in C. Bars, 10 μm.

Ena/VASP proteins are involved downstream of syndecan-2. To further explore this possibility, we examined VASP phosphorylation at the PKA sites in the presence of syndecan-2. Indeed, syndecan-2 overexpression enhanced the phosphorylation levels of VASP in HEK293T cells, as revealed by immunoblotting using phosphopeptide antibodies specifically recognizing PKA-phosphorylated VASP (Fig. 9 B). This data supported the activation of VASP by syndecan-2 overexpression. To address the role of Ena/VASP in syndecan-2–induced filopodia formation, FP4-mito and AP4-mito constructs were coexpressed with syndecan-2 in cells. FP4-mito is a fusion containing EGFP, four binding motifs for Ena/VASP proteins, and a mitochondria target sequence (Bear et al., 2000). This fusion binds and mistargets Ena/VASP protein to mitochondria instead of plasma membrane, reducing the filopodia formation activity of Ena/VASP proteins (Bear et al., 2000; Lebrand et al., 2004). AP4-mito, which contains a mutation in the Ena/VASP-binding motif and fails to interact with Ena/VASP proteins, was used as a negative control. In both HEK293T cells (Fig. S4 B) and cultured hippocampal neurons (Fig. 9, C and D), the expression of FP4-mito reduced syndecan-2–induced filopodia formation. These results supported the notion that Ena/VASP proteins are the downstream mediators of syndecan-2. The addition of FSK into the culture cotransfected with syndecan-2 and FP4-mito did not prevent the blocking effect of FP4-mito in HEK293T cells (Fig. S4 B) or in cultured hippocampal neurons (Fig. 9, C and D), supporting the idea that PKA works upstream of Ena/VASP.

Neurofibromin and Ena/VASP proteins are required for dendritic spine formation

The aforementioned results showed that syndecan-2 promotes filopodia formation via an NF1–PKA–Ena/VASP pathway in both HEK293T cells and cultured hippocampal neurons. To further elucidate the involvement of this signaling pathway in dendritic spine formation, we performed three more experiments. First, we examined the requirement of the cytoplasmic region of syndecan-2 in spine formation. Wild-type syndecan-2, -2ΔC1, and -2Δ3 mutants were transfected into cultured hippocampal neurons at 1 DIV, and their abilities to induce dendritic spine formation were examined at 8–9 DIV. Consistent with previous observations (Ethell and Yamaguchi, 1999), wild-type syndecan-2 induced dendritic spine formation at 8–9 DIV (Fig. 10 A). These spines formed functional synapses because they made contact with presynaptic buttons, as revealed by presynaptic marker synaptophysin staining (Fig. 10 A). For neurons transfected with syndecan-2Δ3, the protrusion density was not significantly different from that of wild-type syndecan-2 ($P = 0.387$; Fig. 10, A and B). However, the majority of the protrusions of syndecan-2Δ3–expressing neurons still carried the characteristics of filopodia (being longer than 2 μm and lacking a head; Fig. 10, A and B), supporting the idea that syndecan-2Δ3 can promote filopodia formation; however, the consequent transformation from filopodia to spines was prevented. For syndecan-2ΔC1, the density of the protrusion was much less than that induced by wild-type syndecan-2 (Fig. 10, A and B). This outcome was similar to the effect of syndecan-2ΔC1 on filopodia formation at 4–5 DIV (Fig. 3 D). These results support the notion that the C1 region of syndecan-2 is required for both filopodia and spine formation and that the C2 region is critical for spine formation. The fact that the protrusion densities induced by syndecan-2 and -2Δ3 were similar (Fig. 10 B) also supports the hypothesis that filopodia are the intermediates of spines in this syndecan-2–dependent process.

Next, we examined the involvement of neurofibromin and Ena/VASP proteins in spine formation by again expressing NF1

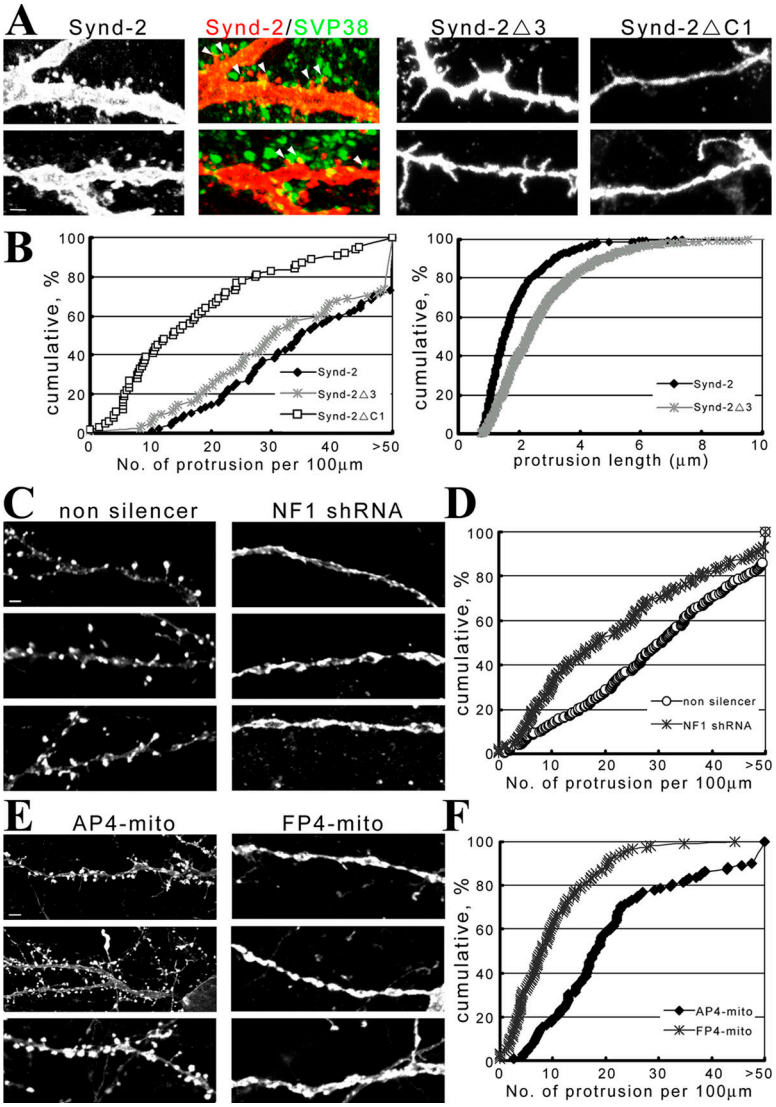

Figure 10. **The syndecan-2–neurofibromin–Ena/VASP signaling pathway is involved in dendritic spinogenesis.** (A, C, and E) Dissociated hippocampal neurons were transfected with syndecan-2, -2△3, or -2△C1 at 1–2 DIV and fixed at 8–9 DIV for immunostaining (A). They were also cotransfected with EGFP-actin and nonsilencer or NF1 shRNA (C) and either DsRed-actin or myc-actin and AP4-mito or FP4-mito at 11–12 DIV and fixed at 16–17 DIV (E). In A, immunostaining using syndecan-2G antibodies was performed to outline the cellular morphology of transfected neurons. Two representative images are shown. For syndecan-2–expressing neurons, double staining with the presynaptic marker synaptophysin (SVP38) was performed. Some of the syndecan-2–induced dendritic spines were adjacent to the SVP38-positive signal, which are marked by arrowheads. In C and E, the EGFP-, DsRed-, or myc-actin patterns were viewed to assess cell morphology. (B) Cumulative probability distributions of A showing the effects of the syndecan-2 cytoplasmic domain on the length and density of dendritic spines. (D) Cumulative probability distributions of C showing the effect of NF1 shRNA on dendritic spine density. (F) Cumulative probability distributions of E showing the effects of FP4-mito on spine density. Bars, 2 μm.

shRNA and FP4-mito constructs, respectively, in hippocampal neurons at 11–12 DIV. The spine density of mature neurons was then examined at 16–17 DIV. Compared with nonsilencer control, the NF1 shRNA construct significantly reduced spine density along dendrites of mature hippocampal neurons ($P < 0.001$; Fig. 10, C and D), supporting the role of neurofibromin in dendritic spine formation. In the investigation targeting Ena/VASP proteins, expression of the FP4-mito construct also inhibited spine formation in mature hippocampal neurons (Fig. 10, E and F), supporting an involvement of Ena/VASP proteins in spine formation. In conclusion, these results indicated that neurofibromin and Ena/VASP proteins contribute to dendritic spine formation, perhaps through the regulation of filopodia formation.

Discussion

Using HEK cells and cultured hippocampal neurons as models, we have demonstrated that the neurofibromin–PKA–Ena/VASP pathway mediates the downstream signaling of syndecan-2. This study shows that syndecan-2 itself can deliver a signal to cells to change cell morphology. Our results also provide the first evidence that both neurofibromin and Ena/VASP proteins are involved in dendritic spine formation.

For cell signaling, syndecans are first identified as coreceptors for growth and differentiation factors. However, the previous studies indicated that syndecans are capable of activating intracellular signaling pathways directly via their short cytoplasmic domains. The first example of this was seen with syndecan-4; overexpression of this protein in CHO cells promotes focal adhesion assembly (Longley et al., 1999). The V region of syndecan-4, which binds to phosphatidylinositol-4,5-bisphosphate and activates PKCα, is critical for this function (Oh et al., 1998). Another study showed that the pleiotrophin/heparin-binding growth-associated molecule, which promotes neurite outgrowth in developing neurons, binds to syndecan-3 to induce a syndecan-3–Src–cortactin interaction (Kinnunen et al., 1998). In the present study, we have demonstrated a third signaling pathway involving a direct interaction of syndecan-2 with the neurofibromin–PKA–Ena/VASP pathway. Overexpression of syndecan-2 induces filopodia formation via PKA activity, which is mediated by neurofibromin, and thus regulates the function of Ena/VASP proteins in filopodia formation. In contrast to the

heparin-binding growth-associated molecule–syndecan-3 pathway, the need for a specific ligand for the activation of syndecan-2 has not been clarified. In our system, overexpression of syndecan-2 is sufficient to induce downstream signaling; however, it cannot be ruled out that an unknown syndecan-2 ligand is present in our culture systems.

Currently, it is also unclear how the overexpression of syndecan-2 enhances the ability of neurofibromin to activate PKA. Perhaps interaction with syndecan-2 changes the conformation of neurofibromin, allowing the activation of adenylyl cyclase. Because syndecans form dimers (and perhaps multimers) via their transmembrane domains and there are two separate syndecan-2–interacting sites in neurofibromin (Hsueh et al., 2001), a single neurofibromin molecule may simultaneously interact with a syndecan-2 dimer. This interaction might fix the neurofibromin molecule in a conformation that favors the activation of adenylyl cyclase. Therefore, increases in the level of syndecan-2 might fix more neurofibromin molecules in a conformation that activates adenylyl cyclase. More investigation is needed to explore this possibility.

The deletion analyses showed that syndecan-2Δ32 and -2ΔC1 mutants were unable to promote filopodia formation. Retention of mutants in the cytoplasm cannot explain this phenotype. Our syndecan-2G antibody recognized the ectodomain of syndecan-2 (unpublished data). It stained both syndecan-2– and -2Δ32–expressing cells in the absence of permeabilization (unpublished data), indicating the normal surface expression of syndecan-2Δ32. Moreover, the expression levels of both syndecan-2ΔC1 and -2Δ32 were comparable with that of wild-type syndecan-2 (Fig. S2 C). The loss of filopodia formation with these mutants is also unlikely to be the result of defects in protein expression or subcellular distribution. It suggests that the regions missing in these deletion constructs are important for filopodia formation.

The current findings indicate that the PKA pathway is essential for syndecan-2–induced filopodia formation. However, PKA activation itself is not sufficient for filopodia formation. It suggests that syndecan-2 overexpression is likely to activate multiple signaling pathways that are all required for dendritic spine formation. Consistent with this speculation, the Ras pathway, which is also regulated by neurofibromin, has been shown to contribute to dendritic spine formation (Wu et al., 2001; Vazquez et al., 2004; Kumar et al., 2005). It is possible that the Ras and PKA pathways downstream of syndecan-2/neurofibromin coordinate and regulate dendritic spinogenesis. Alternatively, the ectodomain of syndecan-2 involved in cell–cell or cell–matrix interaction may also be essential for filopodia outgrowth. Without adhesion via the syndecan-2 ectodomain, filopodial protrusions may not be stable. The observation that overexpression of the entire cytoplasmic domain of syndecan-2 failed to promote filopodia formation (unpublished data) also supports the idea that the ectodomain of syndecan-2 is required in this process. More investigations are required to resolve this issue.

Although the cytoplasmic domain of syndecan-2 is short, it interacts with several proteins. Even the complex formation of neurofibromin, syndecan, and CASK has been shown. However, it is unclear whether there is any cross talk between CASK and neurofibromin. CASK apparently has no influence on the filopodia formation activity of neurofibromin because deletion of the CASK-binding site (EFYA motif) on syndecan-2 did not affect filopodia formation. Instead of being part of the same process, it seems likely that the complex formation of CASK, syndecan-2, and neurofibromin serves to achieve two sequential processes: filopodia formation and dendritic spine maturation. The interaction of syndecan-2 with neurofibromin initiates filopodia formation, and the interaction with CASK may further transform filopodia to dendritic spines. The results of the analysis of cytoplasmic deletion mutants of syndecan-2 in filopodia and spine formation support this speculation.

Ethell et al. (2001) demonstrated that EphB2 receptor tyrosine kinase phosphorylates the tyrosine residues Y189 and Y201 in the C1 and V regions of syndecan-2, respectively. EphB2 phosphorylation is required for syndecan-2 clustering on dendrites and the induction of mature spines. When both of the residues Y189 and Y201 are mutated, the mutant syndecan-2 proteins no longer cluster and promote spinogenesis (Ethell et al., 2001). However, EphB2 phosphorylation seems only to affect spine formation but not filopodia formation because filopodia formation is not affected in neurons expressing syndecan-2 Y189F/Y201F mutant (Ethell et al., 2001). In addition, overexpression of an EphB2 kinase-dead mutant in hippocampal neurons prevents spine but not filopodia formation (Ethell et al., 2001). In addition to tyrosine phosphorylation, the V region of the syndecan-2 cytoplasmic domain contains two PKC phosphorylation sites. *Xenopus laevis* syndecan-2 is phosphorylated by PKC and is critical for establishing left-right asymmetry during early development (Kramer et al., 2002). However, PKC inhibitors did not prevent filopodia formation induced by syndecan-2, suggesting that PKC phosphorylation on the V region only regulates the function of syndecan-2 at an early embryonic stage for left-right decision. Neither EphB2 nor PKC phosphorylation regulates syndecan-2–induced filopodia formation.

In conclusion, our studies show clearly that syndecan-2 plays an active role in delivering a biochemical signal into cells. Syndecan-2 remodels the cytoskeleton and promotes the formation of filopodia via the neurofibromin–PKA–Ena/VASP pathway.

Materials and methods

Hippocampal neuronal culture and analysis of dendritic filopodia/spine formation

Hippocampal neuronal cultures were performed as described previously (Wang et al., 2004; Lin et al., 2006) with the minor modification that 300,000 cells per well were plated in 12-well plates containing poly-L-lysine–coated coverslips in each well. Transfection using calcium phosphate precipitation was performed to deliver the plasmid DNA into neurons. To study the effect of syndecan-2 on filopodia formation, transfection of syndecan-2 was performed at 1–2 DIV, and immunostaining was performed at 4–5 DIV. Filopodia formation was determined by the density of protrusions emerging from neurites with a length between 0.75 and 10 μm. The protrusions longer than 10 μm were recognized as dendritic branches. To study the effect of syndecan-2 on spine formation at 8–9 DIV, the length of individual protrusions and protrusion density were measured. Only the protrusions longer than 0.5 μm were counted. To study intrinsic dendritic spine formation, transfection was performed at 11–12 DIV, and immunofluorescence staining was performed at 16–17 DIV. The densities of protrusions longer than 0.5 μm were determined.

All results were shown in cumulative probability distribution and statistically analyzed using the Kolmogorov-Smirnov test. Significance was determined based on the D and corresponding p-values. All of the data obtained in Kolmogorov-Smirnov tests and sample sizes of each experiment are summarized in the supplemental text (available at http://www.jcb.org/cgi/content/full/jcb.200608121/DC1).

Transfection of COS and HEK cells, immunoblotting, immunoprecipitation, and analysis of filopodia density

The details for transfection of COS cells and immunoblotting of syndecan-2 and neurofibromin have been previously described (Hsueh and Sheng, 1999a,b; Hsueh et al., 2001). The conditions for HEK293T cell transfection using LipofectAMINE (Invitrogen) were identical to those used for COS cells. Immunoprecipitation using COS cell extract was performed as described previously (Hsueh and Sheng, 1999b) with some modifications. In brief, 1 d after transfection, cells were washed twice in PBS and treated with 2 mM dithiobis[succinimidylpropionate] (Pierce Chemical Co.) in PBS at 37°C for 30 min. Free dithiobis[succinimidylpropionate] was then removed by washing twice with PBS. Cells were lysed with radioimmunoprecipitation assay buffer and immunoprecipitated using syndecan-2G antibody. To determine the filopodia density on HEK cell, 24 h after transfection, cells were harvested for immunostaining using syndecan-2G antibodies. Filopodia revealed by syndecan-2G signals on the cell surface were counted and divided by the length of cell circumference. For each treatment, a filopodia density of >50 cells was measured. Cumulative probability distribution was shown, and the Kolmogorov-Smirnov test was used to check the significance. All of the data obtained in Kolmogorov-Smirnov tests and sample sizes of each experiment are summarized in the supplemental text.

Antibodies

A rabbit polyclonal syndecan-2 antibody (syndecan-2G) was generated using a GST–syndecan-2 (residues 33–211) recombinant protein as antigen. The antibody was affinity purified using protein A–Sepharose. The monoclonal antibody against GFP was purchased from Invitrogen. VASP antibody was obtained from BD Biosciences. Antibodies against phosphorylated S157 and S239 of VASP were purchased from Chemicon.

Immunofluorescence analysis and time-lapse study

Cells were washed twice in PBS and fixed in PBS containing 4% PFA and 4% sucrose for 10 min at room temperature. After washing, HEK cells were blocked with 1% BSA/1% normal horse serum, and cultured neurons were blocked with 10% BSA for 1 h. The primary antibody was diluted in PBS containing 0.5% BSA for HEK and PBS containing 3% BSA for neurons and was added to cells for a further 1–2-h incubation. After washing, the AlexaFluor488- or -594–conjugated secondary antibody (Invitrogen) was added and incubated for 1–2 h. Samples were then analyzed at room temperature with either a fluorescence microscope (DM RE; Leica) with a PLAPO 63× NA 1.32 oil objective lens (Leica) or a confocal microscope (LSM510; Carl Zeiss MicroImaging, Inc.) with a plan-Apochromat 63× NA 1.25 oil objective lens (Carl Zeiss MicroImaging, Inc.). For regular fluorescence microscopy, images were acquired with a cooled CCD camera (RTE/CCD-1300-Y/HS; Roper Scientific) operated using MetaMorph software (Molecular Devices). For confocal microscopy, the images were acquired using a laser-scanning microscope system (LSM510; Carl Zeiss MicroImaging, Inc.). Results were then processed for publication using Photoshop software (Adobe) with a minimal adjustment of brightness or contrast applied to the whole images.

For the time-lapse study, syndecan-2 and GFP-actin were cotransfected into HEK293T cells at a ratio of 8:1. 18 h after transfection, the dynamic of syndecan-2–induced filopodia was monitored by GFP-actin pattern in an open chamber under a fluorescence microscope (DMRE; Leica) with an HCX APO 63× 0.90-W water objective lens. Images were acquired with the Roper Scientific cooled CCD camera for at least 10 min. The velocity of the filopodia movement and positions of the filopodia tips were analyzed by MetaMorph software.

Construction of plasmids

Plasmid construction for the mammalian expression of syndecans 1–4 has been previously described (Hsueh et al., 1998). EGFP-Mena, EGFP-VASP, EGFP-EVL, FP4-mito, and AP4-mito constructs (Bear et al., 2000; Loureiro et al., 2002) were provided by F.B. Gertler (Massachusetts Institute of Technology, Cambridge, MA). PKI construct was provided by H.-M. Shih (Institute of Biomedical Science, Academia Sinica, Taipei, Taiwan).

To construct the C-terminal deletion mutants syndecan-2Δ3, -2Δ20, and -2Δ32, the respective syndecan-2 cDNA fragments were PCR amplified and subcloned into the EcoRI site of the vector GW1-cytomegalovirus. The same sense oligonucleotide primer (5′-CGGAATTCAT CGGGTACGAGCCACG-3′) was used for PCR construction of all three mutants. The antisense oligonucleotide primers were as follows: (1) for syndecan-2Δ3, 5′-CGGAATTCCTACTCCTTAGTGGGTGCCTTCT-3′; (2) for syndecan-2Δ20, 5′-CGGAATTCCTAAAGGTCGTAGCTTCCTTCGTCTTTCTTC-3′; and (3) for syndecan-2Δ32, 5′-CGGAATTCCTAGTACACCAACAACAGGATGAG-3′. The underlined sequences are EcoRI sites that were appended for cloning purposes. To construct the syndecan-2ΔC1 mutant, a pair of primers (5′-CGGGTACCATGCGGGTACGAGCCACG-3′ and 5′-GTACACCAACAACAGGATGAG-3′) were used to amplify the region containing the extracellular and transmembrane domains. A pair of primers (5′-GACCTTGGAGAACGCAAACCG-3′ and 5′-CGGAATTCTTATGCATAAAACTCCTTAGT-3′) was used to amplify the variable and C2 domains. These two fragments were ligated by blunt-end ligation and subcloned into the KpnI and EcoRI sites of the vector GW1-cytomegalovirus. A QuikChange XL Site-Directed Mutagenesis kit (Stratagene) was used for generating the syndecan-2 RK/AA, KD/AA, and silent mutants. For syndecan-2 RK/AA, the pair of primers 5′-GTTGGTGTACCGCATGGCGGCGAAAGACGAAGGAAGCTAC-3′ and 5′-GCTTCCTTCGTCTTTCGCCGCCATGCGGTACACCAACAAC-3′ was used for site-directed mutagenesis. For syndecan-2 KD/AA, the primers 5′-GTACCGCATGCGGAAGGCAGCCGAAGGAAGCTACGACCTTG-3′ and 5′-GTCGTAGCTTCCTTCGGCTGCCTTCCGCATGCGGTACAC-3′ were used. For the syndecan-2 silent mutant, the pair of primers 5′-AGCAGCTCCATTGAGGAAGCTTCAGGGTTGTATCCTATTG-3′ and 5′-C AATAGGATACAACCCTGAAGCTTC-3′ was used. The underlined residues indicate the mutated sites.

For vector-based syndecan-2 RNAi construction, a pair of oligonucleotides (syndecan-2is, 5′-GATCCCCGCTTCAGGATTATATCCTATTCAAGAGATAGGATATAATCCTGAAGCTTTTTGGAAA-3′; syndecan-2iAs, 5′-GCTTTTCCAAAAAGCTTCAGGATTATATCCTATCTCTTGAATAGGATATAATCCTGAAGCGGG-3′) was annealed and inserted into the BglII and HindIII sites of the siRNA expression vector pSUPER.neo+GFP (OligoEngine). The underlined residues correspond to the nucleotide residues 148–166 of rat syndecan-2 cDNA. The NF1 shRNA expression constructs 27 and 32 in vector pSM2c were purchased from Open Biosystems and corresponded to the nucleotide residues 8,416–8,436 and 3,349–3,370 of human type I NF1, respectively. Because residues 8,416–8,436 are identical in the human and rat NF1 genes, construct 27 can also knock down rat NF1. Nonsilencer control expressing and shRNA sharing no homology with any known mammalian genes were also purchased from Open Biosystems. The Jn and Pn mammalian expression constructs were created by excising the Jn and Pn fragments from the Jn-pGAD10 and Pn-pGAD10 constructs (Hsueh et al., 2001) with EcoRI and subcloning them into the EcoRI site of a modified vector GW1 containing a myc cassette. Plasmids EGFP and EGFP-actin were purchased from CLONTECH Laboratories, Inc. For myc-tagged actin, actin cDNA was digested from EGFP-actin and subcloned into the BglII site of the vector myc-GW1.

PKA activity assay

HEK293T cells were transfected with the vector control or a variety of syndecan-2 constructs. 18 h after transfection, cells were harvested for PKA activity analysis using an ELISA kit from Calbiochem. Equal protein amounts of cell extracts were used.

Animals and housing

All animal experiments were performed with the approval of and in strict accordance with the guidelines of the Academia Sinica Institutional Animal Care and Utilization Committee and the Republic of China Council of Agriculture Guidebook for the Care and Use of Laboratory Animals. Pregnant rats were housed individually and killed by CO_2 inhalation. All efforts were made to minimize animal suffering and to reduce the number of animals required.

Online supplemental material

Fig. S1 is the characterization of syndecan-2 and neurofibromin RNAi constructs and the dominant-negative mutant of neurofibromin. Fig. S2 shows the specificity of syndecan-2 antibody and expression of syndecan-2 wild-type and mutant constructs. Fig. S3 shows that PKC and PI3K are not involved in filopodia formation downstream of syndecan-2. Fig. S4 shows that Ena/VASP proteins are the downstream effectors of PKA activated by syndecan-2 in HEK293T cells. Supplemental text contains the data obtained in Kolmogorov-Smirnov tests, including D and corresponding p-values and sample sizes of each experiment. Online supplemental material is available at http://www.jcb.org/cgi/content/full/jcb.200608121/DC1.

We thank Dr. Frank B. Gertler for Ena/VASP constructs, Dr. Hsiu-Ming Shih for the PKI construct, Sue-Ping Lee for technical assistance on confocal analysis, and Dr. Harry Wilson for English language editing.

This work was supported by grants from Academia Sinica, the National Science Council (NSC94-2321-B-001-022 and NSC 95-2321-B-001-013 to Y.-P. Hsueh), and the National Health Research Institute (NHRI-EX94-9403NI and NHRI-EX95-9403NI to Y.-P. Hsueh).

Submitted: 21 August 2006
Accepted: 4 May 2007

References

Acosta, M.T., G.A. Gioia, and A.J. Silva. 2006. Neurofibromatosis type 1: new insights into neurocognitive issues. *Curr. Neurol. Neurosci. Rep.* 6:136–143.

Aszodi, A., A. Pfeifer, M. Ahmad, M. Glauner, X.H. Zhou, L. Ny, K.E. Andersson, B. Kehrel, S. Offermanns, and R. Fassler. 1999. The vasodilator-stimulated phosphoprotein (VASP) is involved in cGMP- and cAMP-mediated inhibition of agonist-induced platelet aggregation, but is dispensable for smooth muscle function. *EMBO J.* 18:37–48.

Bear, J.E., J.J. Loureiro, I. Libova, R. Fassler, J. Wehland, and F.B. Gertler. 2000. Negative regulation of fibroblast motility by Ena/VASP proteins. *Cell*. 101:717–728.

Bear, J.E., T.M. Svitkina, M. Krause, D.A. Schafer, J.J. Loureiro, G.A. Strasser, I.V. Maly, O.Y. Chaga, J.A. Cooper, G.G. Borisy, and F.B. Gertler. 2002. Antagonism between Ena/VASP proteins and actin filament capping regulates fibroblast motility. *Cell*. 109:509–521.

Beauvais, D.M., B.J. Burbach, and A.C. Rapraeger. 2004. The syndecan-1 ectodomain regulates alphavbeta3 integrin activity in human mammary carcinoma cells. *J. Cell Biol.* 167:171–181.

Carlisle, H.J., and M.B. Kennedy. 2005. Spine architecture and synaptic plasticity. *Trends Neurosci.* 28:182–187.

Cichowski, K., and T. Jacks. 2001. NF1 tumor suppressor gene function: narrowing the GAP. *Cell*. 104:593–604.

Cohen, A.R., D.F. Woods, S.M. Marfatia, Z. Walther, A.H. Chishti, J.M. Anderson, and D.F. Wood. 1998. Human CASK/LIN-2 binds syndecan-2 and protein 4.1 and localizes to the basolateral membrane of epithelial cells. *J. Cell Biol.* 142:129–138.

Costa, R.M., and A.J. Silva. 2002. Molecular and cellular mechanisms underlying the cognitive deficits associated with neurofibromatosis 1. *J. Child Neurol*. 17:622–6.

Costa, R.M., N.B. Federov, J.H. Kogan, G.G. Murphy, J. Stern, M. Ohno, R. Kucherlapati, T. Jacks, and A.J. Silva. 2002. Mechanism for the learning deficits in a mouse model of neurofibromatosis type 1. *Nature*. 415:526–530.

Dasgupta, B., L.L. Dugan, and D.H. Gutmann. 2003. The neurofibromatosis 1 gene product neurofibromin regulates pituitary adenylate cyclase-activating polypeptide-mediated signaling in astrocytes. *J. Neurosci.* 23:8949–8954.

Ethell, I.M., and E.B. Pasquale. 2005. Molecular mechanisms of dendritic spine development and remodeling. *Prog. Neurobiol.* 75:161–205.

Ethell, I.M., and Y. Yamaguchi. 1999. Cell surface heparan sulfate proteoglycan syndecan-2 induces the maturation of dendritic spines in rat hippocampal neurons. *J. Cell Biol.* 144:575–586.

Ethell, I.M., K. Hagihara, Y. Miura, F. Irie, and Y. Yamaguchi. 2000. Synbindin, a novel syndecan-2-binding protein in neuronal dendritic spines. *J. Cell Biol.* 151:53–68.

Ethell, I.M., F. Irie, M.S. Kalo, J.R. Couchman, E.B. Pasquale, and Y. Yamaguchi. 2001. EphB/syndecan-2 signaling in dendritic spine morphogenesis. *Neuron*. 31:1001–1013.

Filla, M.S., P. Dam, and A.C. Rapraeger. 1998. The cell surface proteoglycan syndecan-1 mediates fibroblast growth factor-2 binding and activity. *J. Cell. Physiol.* 174:310–321.

Gao, Y., M. Li, W. Chen, and M. Simons. 2000. Synectin, syndecan-4 cytoplasmic domain binding PDZ protein, inhibits cell migration. *J. Cell. Physiol.* 184:373–379.

Geese, M., J.J. Loureiro, J.E. Bear, J. Wehland, F.B. Gertler, and A.S. Sechi. 2002. Contribution of Ena/VASP proteins to intracellular motility of listeria requires phosphorylation and proline-rich core but not F-actin binding or multimerization. *Mol. Biol. Cell*. 13:2383–2396.

Granes, F., R. Garcia, R.P. Casaroli-Marano, S. Castel, N. Rocamora, M. Reina, J.M. Urena, and S. Vilaro. 1999. Syndecan-2 induces filopodia by active cdc42Hs. *Exp. Cell Res.* 248:439–456.

Granes, F., J.M. Urena, N. Rocamora, and S. Vilaro. 2000. Ezrin links syndecan-2 to the cytoskeleton. *J. Cell Sci.* 113:1267–1276.

Grootjans, J.J., P. Zimmermann, G. Reekmans, A. Smets, G. Degeest, J. Durr, and G. David. 1997. Syntenin, a PDZ protein that binds syndecan cytoplasmic domains. *Proc. Natl. Acad. Sci. USA*. 94:13683–13688.

Hannan, F., I. Ho, J.J. Tong, Y. Zhu, P. Nurnberg, and Y. Zhong. 2006. Effect of neurofibromatosis type I mutations on a novel pathway for adenylyl cyclase activation requiring neurofibromin and Ras. *Hum. Mol. Genet.* 15:1087–1098.

Hauser, W., K.P. Knobeloch, M. Eigenthaler, S. Gambaryan, V. Krenn, J. Geiger, M. Glazova, E. Rohde, I. Horak, U. Walter, and M. Zimmer. 1999. Megakaryocyte hyperplasia and enhanced agonist-induced platelet activation in vasodilator-stimulated phosphoprotein knockout mice. *Proc. Natl. Acad. Sci. USA*. 96:8120–8125.

Hering, H., and M. Sheng. 2001. Dendritic spines: structure, dynamics and regulation. *Nat. Rev. Neurosci.* 2:880–888.

Hsueh, Y.P., and M. Sheng. 1999a. Regulated expression and subcellular localization of syndecan heparan sulfate proteoglycans and the syndecan-binding protein CASK/LIN-2 during rat brain development. *J. Neurosci.* 19:7415–7425.

Hsueh, Y.P., and M. Sheng. 1999b. Requirement of N-terminal cysteines of PSD-95 for PSD-95 multimerization and ternary complex formation, but not for binding to potassium channel Kv1.4. *J. Biol. Chem.* 274:532–536.

Hsueh, Y.P., F.C. Yang, V. Kharazia, S. Naisbitt, A.R. Cohen, R.J. Weinberg, and M. Sheng. 1998. Direct interaction of CASK/LIN-2 and syndecan heparan sulfate proteoglycan and their overlapping distribution in neuronal synapses. *J. Cell Biol.* 142:139–151.

Hsueh, Y.P., A.M. Roberts, M. Volta, M. Sheng, and R.G. Roberts. 2001. Bipartite interaction between neurofibromatosis type I protein (neurofibromin) and syndecan transmembrane heparan sulfate proteoglycans. *J. Neurosci.* 21:3764–3770.

Kinnunen, T., M. Kaksonen, J. Saarinen, N. Kalkkinen, H.B. Peng, and H. Rauvala. 1998. Cortactin-Src kinase signaling pathway is involved in N-syndecan-dependent neurite outgrowth. *J. Biol. Chem.* 273:10702–10708.

Klass, C.M., J.R. Couchman, and A. Woods. 2000. Control of extracellular matrix assembly by syndecan-2 proteoglycan. *J. Cell Sci.* 113:493–506.

Kramer, K.L., J.E. Barnette, and H.J. Yost. 2002. PKCgamma regulates syndecan-2 inside-out signaling during *Xenopus* left-right development. *Cell*. 111:981–990.

Kumar, V., M.X. Zhang, M.W. Swank, J. Kunz, and G.Y. Wu. 2005. Regulation of dendritic morphogenesis by Ras-PI3K-Akt-mTOR and Ras-MAPK signaling pathways. *J. Neurosci.* 25:11288–11299.

Lanier, L.M., M.A. Gates, W. Witke, A.S. Menzies, A.M. Wehman, J.D. Macklis, D. Kwiatkowski, P. Soriano, and F.B. Gertler. 1999. Mena is required for neurulation and commissure formation. *Neuron*. 22:313–325.

Laurent, V., T.P. Loisel, B. Harbeck, A. Wehman, L. Grobe, B.M. Jockusch, J. Wehland, F.B. Gertler, and M.F. Carlier. 1999. Role of proteins of the Ena/VASP family in actin-based motility of *Listeria monocytogenes*. *J. Cell Biol.* 144:1245–1258.

Lebrand, C., E.W. Dent, G.A. Strasser, L.M. Lanier, M. Krause, T.M. Svitkina, G.G. Borisy, and F.B. Gertler. 2004. Critical role of Ena/VASP proteins for filopodia formation in neurons and in function downstream of netrin-1. *Neuron*. 42:37–49.

Lin, C.W., T.N. Huang, G.S. Wang, T.Y. Kuo, T.Y. Yen, and Y.P. Hsueh. 2006. Neural activity- and development-dependent expression and distribution of CASK interacting nucleosome assembly protein in mouse brain. *J. Comp. Neurol.* 494:606–619.

Lippman, J., and A. Dunaevsky. 2005. Dendritic spine morphogenesis and plasticity. *J. Neurobiol.* 64:47–57.

Longley, R.L., A. Woods, A. Fleetwood, G.J. Cowling, J.T. Gallagher, and J.R. Couchman. 1999. Control of morphology, cytoskeleton and migration by syndecan-4. *J. Cell Sci.* 112:3421–3431.

Loureiro, J.J., D.A. Rubinson, J.E. Bear, G.A. Baltus, A.V. Kwiatkowski, and F.B. Gertler. 2002. Critical roles of phosphorylation and actin binding motifs, but not the central proline-rich region, for Ena/vasodilator-stimulated phosphoprotein (VASP) function during cell migration. *Mol. Biol. Cell*. 13:2533–2546.

Oh, E.S., A. Woods, S.T. Lim, A.W. Theibert, and J.R. Couchman. 1998. Syndecan-4 proteoglycan cytoplasmic domain and phosphatidylinositol 4,5-bisphosphate coordinately regulate protein kinase C activity. *J. Biol. Chem.* 273:10624–10629.

Reiland, J., R.D. Sanderson, M. Waguespack, S.A. Barker, R. Long, D.D. Carson, and D. Marchetti. 2004. Heparanase degrades syndecan-1 and perlecan heparan sulfate: functional implications for tumor cell invasion. *J. Biol. Chem.* 279:8047–8055.

Rosser, T.L., and R.J. Packer. 2003. Neurocognitive dysfunction in children with neurofibromatosis type 1. *Curr. Neurol. Neurosci. Rep.* 3:129–136.

Tada, T., and M. Sheng. 2006. Molecular mechanisms of dendritic spine morphogenesis. *Curr. Opin. Neurobiol.* 16:95–101.

Tong, J., F. Hannan, Y. Zhu, A. Bernards, and Y. Zhong. 2002. Neurofibromin regulates G protein-stimulated adenylyl cyclase activity. *Nat. Neurosci.* 5:95–96.

Vazquez, L.E., H.J. Chen, I. Sokolova, I. Knuesel, and M.B. Kennedy. 2004. SynGAP regulates spine formation. *J. Neurosci.* 24:8862–8872.

Wang, G.S., C.J. Hong, T.Y. Yen, H.Y. Huang, Y. Ou, T.N. Huang, W.G. Jung, T.Y. Kuo, M. Sheng, T.F. Wang, and Y.P. Hsueh. 2004. Transcriptional modification by a CASK-interacting nucleosome assembly protein. *Neuron.* 42:113–128.

Wu, G.Y., K. Deisseroth, and R.W. Tsien. 2001. Spaced stimuli stabilize MAPK pathway activation and its effects on dendritic morphology. *Nat. Neurosci.* 4:151–158.

Yunoue, S., H. Tokuo, K. Fukunaga, L. Feng, T. Ozawa, T. Nishi, A. Kikuchi, S. Hattori, J. Kuratsu, H. Saya, and N. Araki. 2003. Neurofibromatosis type I tumor suppressor neurofibromin regulates neuronal differentiation via its GTPase-activating protein function toward Ras. *J. Biol. Chem.* 278:26958–26969.

Zhu, Y., and L.F. Parada. 2001. Neurofibromin, a tumor suppressor in the nervous system. *Exp. Cell Res.* 264:19–28.